JOURNAL OF MATERIALS SCIENCE 37 (2002) 2975–2982

Temperature dependence of flexural strength and microstructure of $Al_2O_3/Y_3Al_5O_{12}/ZrO_2$ ternary melt growth composites

Y. WAKU*, S. SAKATA*, A. MITANI*, K. SHIMIZU*
Japan Ultra-High Temperature Materials Research Institute, 573-3 Okiube, Ube City, Yamaguchi, 755-0001 Japan
E-mail: 25222u@ube-ind.co.jp

M. HASEBE
Department of Materials Science and Engineering, Kyushu Institute of Technology, Sensui-cho, Tobata-ku, Kitakyushu, 804-8650 Japan

New $Al_2O_3/Y_3Al_5O_{12}$(YAG)/ZrO_2 ternary Melt Growth Composites (MGCs) with a novel microstructure have been fabricated by unidirectional solidification. These MGCs displayed superior high-temperature strength characteristics. The flexural strength increases progressively in the range 650–800 MPa with a rise in temperature from room temperature up to 1873 K. These excellent high-temperature characteristics are closely linked to such factors as: a microstructure consisting of three-dimensionally continuous and complexly entangled single-crystal Al_2O_3 with a hexagonal structure, single-crystal YAG with a garnet structure and fine ZrO_2 with a cubic structure; characteristic dimensions of the microstructure of Al_2O_3/YAG/ZrO_2 ternary eutectic ceramics of around 2–3 μm for YAG, around 2–3 μm for Al_2O_3 and around 0.4–0.8 μm for ZrO_2; and the fact that no amorphous phase is formed at interfaces between any of the phases.

1. Introduction

A 1% improvement in thermal efficiency would lead to a worldwide annual saving in energy costs of around $1000 billion [1]. Accordingly, studies all over the world are seeking to develop ultra-high-temperature structural materials that will improve thermal efficiency in aircraft engines and other high-efficiency gas turbines. Research is being vigorously pursued into the development of very high temperature structural materials that remain stable under use for prolonged periods in an oxidizing atmosphere at very high temperatures. Microstructural studies on an $Al_2O_3/Y_3Al_5O_{12}$(YAG) system produced using the Bridgman method showed that the microstructure of the composite could be controlled by unidirectional solidification [2]. As a candidate high-temperature structural material, it has been reported that a unidirectionally solidified Al_2O_3/YAG eutectic composite has superior flexural strength, thermal stability and creep resistance at high temperatures [3–5]. Superior mechanical properties at high temperature of small diameters rods from the $Al_2O_3/ZrO_2(Y_2O_3)$ system have also been reported by Sayir *et al*. [6] and Paster *et al*. [7].

Waku *et al*. [8–13] have recently developed Al_2O_3/YAG and $Al_2O_3/Er_3Al_5O_{12}$ (EAG) binary MGCs by unidirectional solidification. The MGCs are thermally stable and have the following properties: (1) maintenance of the flexural strength at room temperature almost up to the melting point, (2) a compression creep strength at 1873 K and a strain rate of 10^{-4} s^{-1} which is 7–13 times higher than that of sintered composites with the same composition, (3) no weight gain or grain growth even when heated at 1973 K in an air atmosphere for 1000 hours. However, the flexural strength of these binary MGCs from room temperature to high temperatures is low.

To increase the high-temperature flexural strength of a representative Al_2O_3/YAG binary MGC, a Al_2O_3/YAG/ZrO_2 ternary MGC has been fabricated with a high flexural strength by microstructural refining using a eutectic reaction of the $Al_2O_3/Y_2O_3/ZrO_2$ ternary system[14]. In this paper the flexural strength of the Al_2O_3/YAG/ZrO_2 ternary MGC as a function of testing temperature is compared with *a*-axis sapphire and a Al_2O_3/YAG/ZrO_2 sintered composite.

2. Experimental

2.1. Manufacture of powder blends

Commercially available Al_2O_3 powder (AKP-30, Sumitimo Chemical Co., Ltd., Tokyo, Japan), Y_2O_3

Present Address: Ube Research Laboratory, Corporate Research & Development, UBE Industries Ltd., 1978-5 Kogushi, Ube City, Yamaguchi, 755-8633 Japan.

powder (Y_2O_3-RU, submicron-type, Shin-etsu Chemical Co., Ltd., Tokyo, Japan) and ZrO_2 powder (TZ-O, Tosoh Co., Ltd., Tokyo, Japan) were mixed to give molar ratios of $Al_2O_3/Y_2O_3 = 82/18$ and $Al_2O_3/Y_2O_3/ZrO_2 = 71.1/16.8/12.1$, 69.7/16.5/13.8, 68.3/16.2/15.5, 67.1/15.9/17.1, 65.8/15.6/18.6 and 64.6/15.3/20.1. Wet ball milling using ethanol was carried out to obtain homogeneous powder mixtures.

2.2. Unidirectional solidification

All unidirectional solidification experiments were performed using the advanced-alloy crystalline-structure-controlling equipment at the Japan Ultra-high Temperature Materials Research Center. The mixed powders were melted in a Mo crucible heated by high-frequency induction heating under a pressure of 1.3×10^{-3} Pa of argon, and then, after holding for 30 minutes at 2173 K, unidirectional solidification was carried out by lowering the Mo crucible at a speed of 30 mm h^{-1} in the same argon atmosphere. For accurate control of crystal growth, a mini-crucible (2 mm in diameter and 17 mm in length) for growing a suitable seed crystal was set at the bottom of the main crucible.

2.3. Sintering

Some of the mixed powder ($Al_2O_3 + Y_2O_3 + ZrO_2$) was not treated as described above, but was hot-pressed in a carbon die for 1 hour at 1923 K in vacuum (1.3 Pa) to fabricate a sintered $Al_2O_3/YAG/ZrO_2$ composite of dimensions 50 mm × 60 mm × 5 mm. This sintered composite had the same composition as the $Al_2O_3/YAG/ZrO_2$ ternary MGC.

2.4. Evaluation of mechanical properties

Three-point flexural tests were carried out using specimens of dimensions of 3 mm × 4 mm × 36 mm with the long axis parallel to the solidification direction. The equipment used in this study was the high-temperature uniaxial tension, compression and bending test system (a modified creep and fatigue machine, Instron type 8562). Flexural tests were conducted at 1873 K in an argon gas atmosphere at a crosshead speed of 0.5 mm min^{-1}. The measurement of fracture toughness was performed according to ASTM E399-90 [15] at room temperature using the same machine as for the flexural tests. The dimensions of single edge-notched specimens were 2 mm × 4 mm × 25 mm. A 2 mm notch was introduced using a diamond wheel. The radius of the notch-tip was 10 μm. Fracture toughness was calculated using the following equation:

$$K_{\mathrm{Ic}} = (PS)/(Bw^{3/2}) f(a/w)$$

$$f(a/w) = 3(a/w)^{1/2}[1.99 - (a/w)(1 - a/w) \times (2.15 - 3.97a/w + 2.7a^2/w^2)]/[2(1 + 2a/w)(1 - a/w)^{2/3}]$$

Where, P is the load, S is the span, B is the specimen thickness, w is the specimen width and a is a notch length.

Structural analyses were undertaken using a Rigaku-Denki RAD-RB X-ray diffractometer. Transmission electron microscopy (TEM) observations of the interfaces and grain-boundary structures were conducted using a Japan Electron JEM-2010. Electron probe microanalyses (EPMA) were undertaken using a Japan Electron JMX-8621MX.

3. Results and discussion

3.1. Computer simulation of a liquidus surface in $Al_2O_3/Y_2O_3/ZrO_2$ ternary equilibrium diagram

All equilibrium calculations were performed using the computer program Thermo-calc that was originally developed by Thermo-Calc Software Co. This computer program is based on the principle of minimization of the Gibbs free energy of the system. The thermodynamic parameters necessary for calculating a ternary liquidus surface were estimated from comparison of calculated binary phase diagrams with experimental Al_2O_3/Y_2O_3 binary [16], Al_2O_3/ZrO_2 binary [17] and Y_2O_3/ZrO_2 binary [18] diagrams. The main objective of computer simulation in this study is to obtain a liquidus surface diagram by employing the CALPHAD (calculation of phase diagram) method, thus several complex solid phase transformations in the Y_2O_3/ZrO_2 binary system are neglected. Fig. 1 shows a calculated liquidus surface diagram in $Al_2O_3/Y_2O_3/ZrO_2$ ternary equilibrium system. It is found that there are five ternary eutectic compositions [a, b, c, d and e in Fig. 1.]

In the case of $Al_2O_3/Y_2O_3/ZrO_2 = 71.1/16.8/12.1$ molar ratio (eutectic composition 'a' in Fig. 1), no cracks were observed in the unidirectionally solidified composite. Therefore, this composition system may be produced *in situ* by the unidirectional solidification process, with the composite consisting of Al_2O_3, YAG and ZrO_2. Referring to eutectic composition 'a' in Fig. 1, several compositional experiments were conducted, increasing the amount of ZrO_2. As a result, it was clear that the exact ternary composition for the eutectic reaction is $Al_2O_3/Y_2O_3/ZrO_2 = 65.8/15.6/18.6$ mole ratio which is slightly different from the composition "a" in Fig. 1.

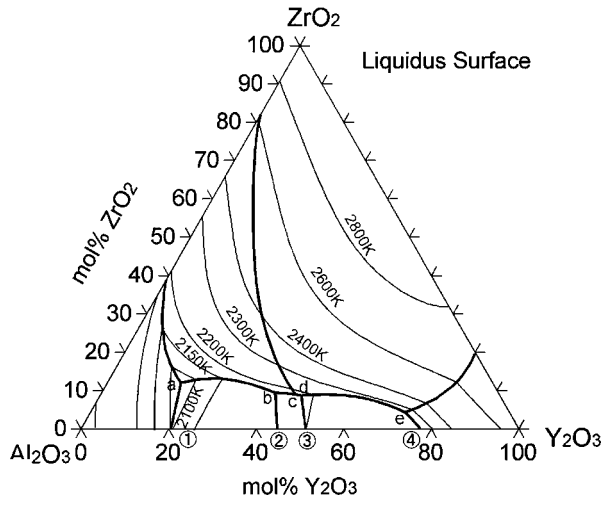

Figure 1 A liquidus surface diagram in $Al_2O_3/Y_2O_3/ZrO_2$ ternary equilibrium system calculated by the computer using the CALPHAD method.

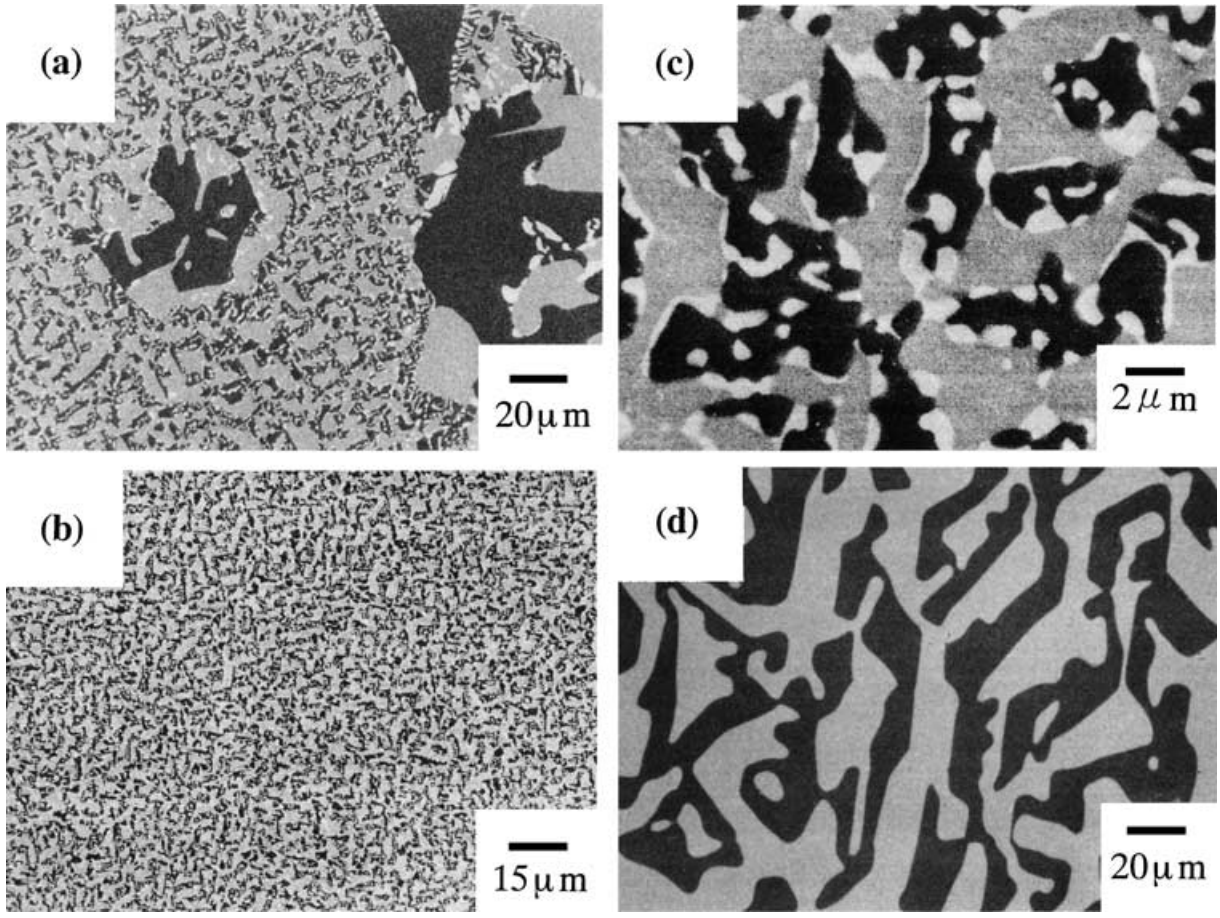

Figure 2 SEM images showing the microstructure of a cross-section perpendicular to the solidification direction of the unidirectionally solidified composites. (a) Al_2O_3/YAG/ZrO_2 ternary hypoeutectic composites, (b) and (c) Al_2O_3/YAG/ZrO_2 ternary MGC, (d) Al_2O_3/YAG binary MGCs. (c) an enlarged image of (b).

3.2. Microstructure

Fig. 2a–c show SEM images of the cross-section perpendicular to the solidification direction of the Al_2O_3/YAG/ZrO_2 ternary composites. For comparison, a SEM image of the Al_2O_3/YAG binary MGC is also shown in Fig. 2d. The microstructures of the ternary composites consisted of Al_2O_3, YAG and Y-containing fully stabilized cubic ZrO_2 ($Zr_{0.72}Y_{0.28}O_{1.86}$, described as cubic-$ZrO_2$ in the following), as determined from X-ray diffraction. The Microstructure of the unidirectionally solidified ternary hypoeutectic composite with a molar ratio of $ZrO_2 < 18.6$ (Fig. 2a) consists of a large primary crystal, which is Al_2O_3/YAG binary eutectic, and a fine Al_2O_3/YAG/ZrO_2 ternary eutectic. The dimensions of the primary crystal are nearly the same as that in an Al_2O_3/YAG binary MGC (Fig. 2d). The volume of primary crystal decreases with increasing ZrO_2.

When the molar ratio of ZrO_2 becomes 18.6 a fine and uniform microstructure consisting of only Al_2O_3/YAG/ZrO_2 ternary eutectic as shown in Fig. 2b and c is obtained. The large gray plate-like area in the SEM micrograph is the YAG phase, the dark area is the Al_2O_3 phase and the fine light area in the Al_2O_3 phase is the cubic-ZrO_2phase as shown in Fig. 2c (identified by X-ray diffraction and EPMA analysis). The dimension of the YAG phase in the Al_2O_3/YAG/ZrO_2 ternary MGCs is around 2–3 μm (this dimension is defined as the typical length of the short axis of each domain seen in the cross-section perpendicular to the solidification direction) i.e., smaller by a factor of 10 than the 20–30 μm of the Al_2O_3/YAG binary MGC [8, 11]. Much of the cubic-ZrO_2 exists at interfaces between Al_2O_3 and YAG or in Al_2O_3, it seldom exists in YAG. The dimension of the fine cubic-ZrO_2 is 0.4–0.8 μm. Homogeneous microstructures with no pores or colonies are observed in both binary and ternary MGCs (Fig. 2c and d).

In the X-ray diffraction pattern for the ternary MGC, diffraction peaks from the (300) plane of the Al_2O_3 phase, from the (400)(800) planes of the YAG phase and from the (200)(400) planes of the cubic-ZrO_2 phase are the only ones observed from the plane perpendicular to the solidification direction. Consequently, it can be concluded that this ternary MGC consists of $\langle\bar{2}10\rangle$ single-crystal Al_2O_3 with a hexagonal structure, $\langle 100\rangle$ single-crystal YAG with a garnet structure and $\langle 100\rangle$ single-crystal ZrO_2 with a cubic structure.

3.3. Interface

The existence of amorphous phases at interfaces or grain boundaries generally leads to a reduction in the strength of the material at high temperatures [19, 20]. Fig. 3a–c show typical high-resolution TEM images of the interfaces between Al_2O_3 and YAG, YAG and cubic-ZrO_2, Al_2O_3 and cubic-ZrO_2 respectively in the present ternary MGC. No amorphous phases are observed at any of the interfaces and relatively compatible interfaces are formed.

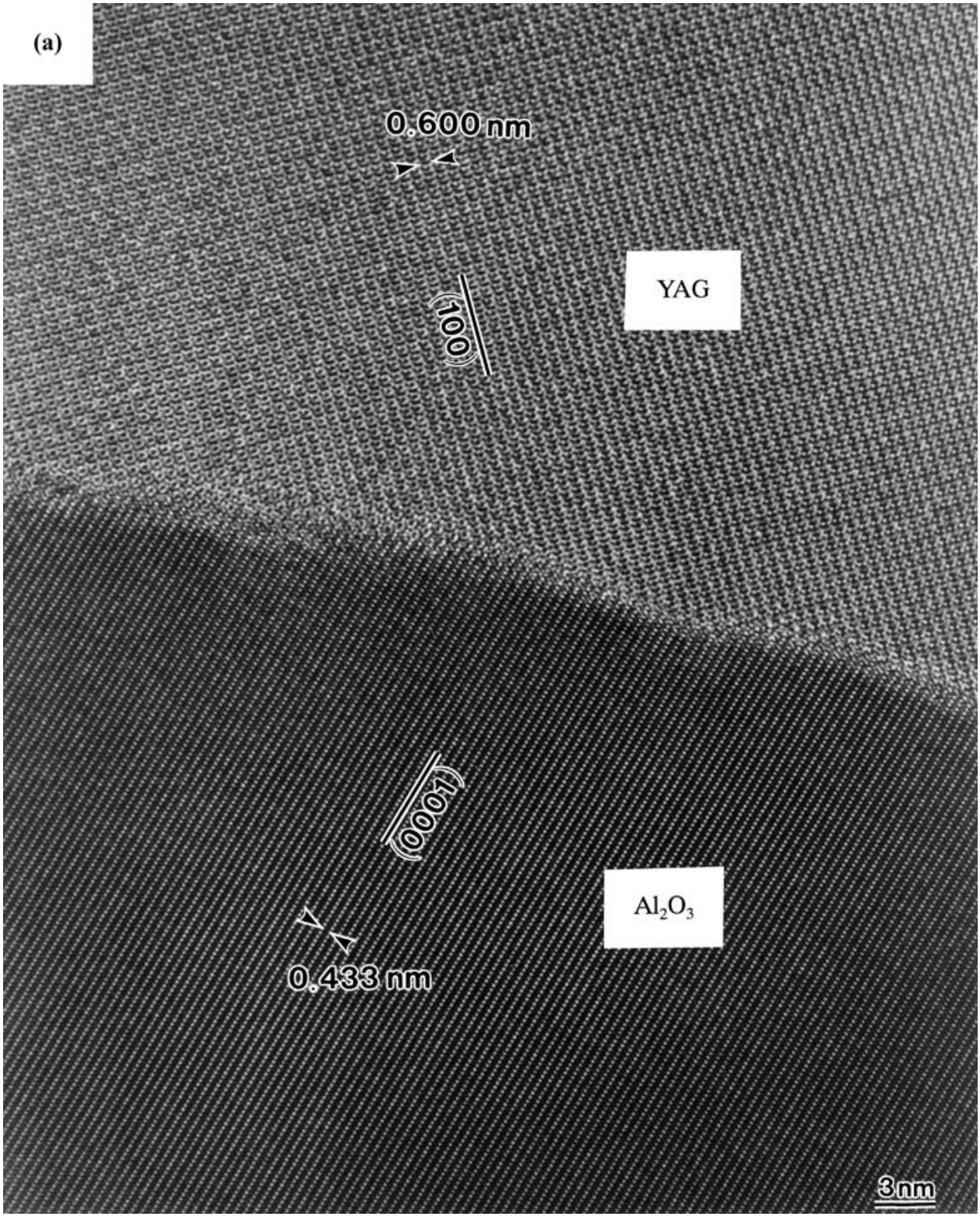

Figure 3 High-resolution TEM micrographs showing (a) the interface between Al_2O_3 and YAG phases, (b) the interface between YAG and cubic-ZrO_2 phases and (c) the interface between cubic-ZrO_2 and Al_2O_3 phases in the Al_2O_3/YAG/ZrO_2 ternary MGC. The beam directions are [1$\bar{1}$2] Al_2O_3, [001] YAG and [013] ZrO_2 for (a), (b) and (c). (*Continued.*)

3.4. Three-dimensional configurations of the microstructure

Fig. 4 shows a SEM micrograph which illustrates the three-dimensional configuration of the single-crystal YAG and the cubic-ZrO_2 phase in the ternary MGC from which Al_2O_3 had been removed by heating in graphite powder at 1923 K for 2 hours. The configuration of single-crystal YAG and fine cubic-ZrO_2 phases is a three-dimensionally connected porous structure, of irregular shape. It can be concluded that the ternary MGC has a microstructure consisting of three-dimensionally continuous and complexly entangled single-crystal Al_2O_3, single crystal YAG and fine cubic-ZrO_2 phases. This microstructure was fabricated by controlling accurately crystal growth and the solidification process in the unidirectional solidification.

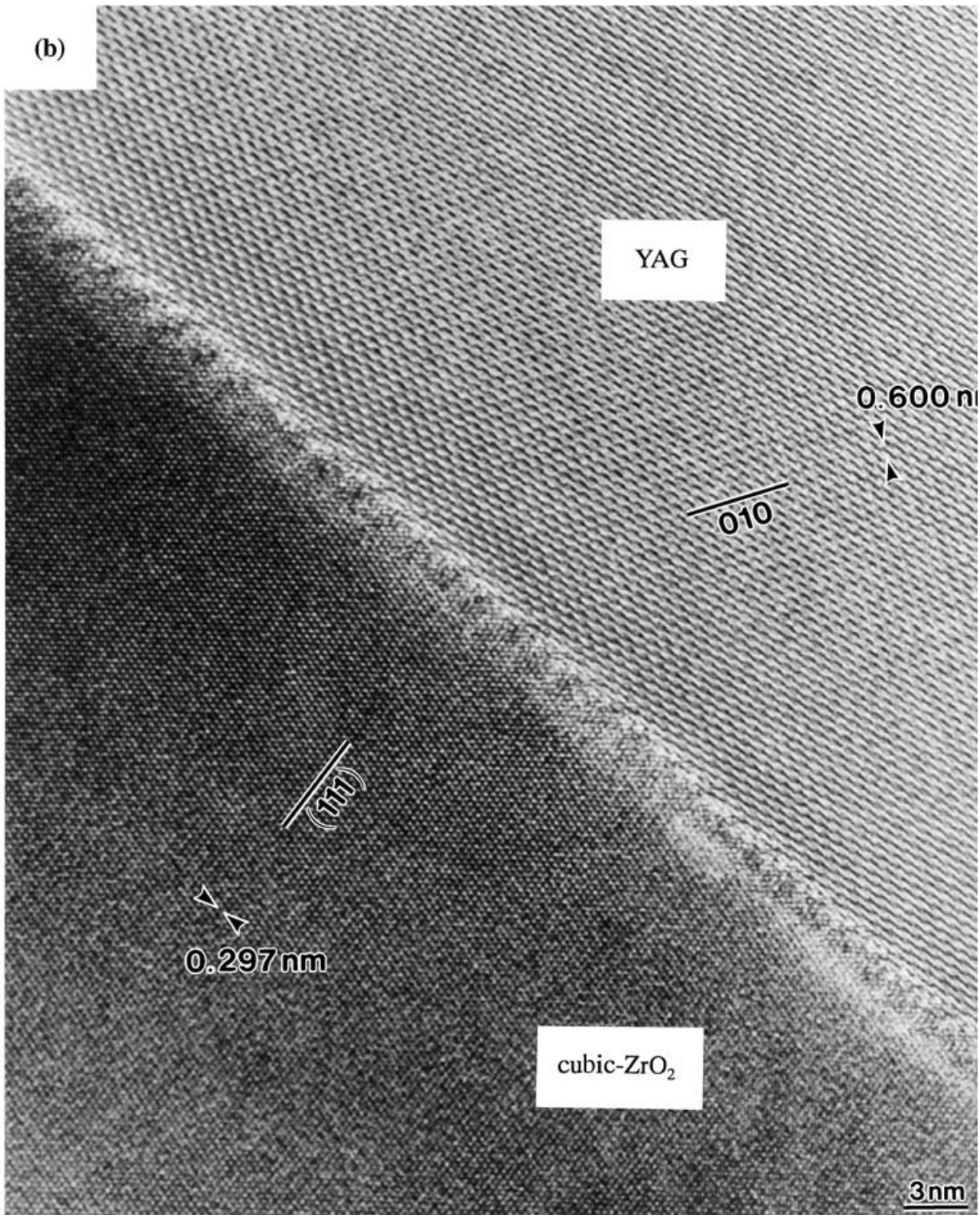

Figure 3 (*Continued.*)

3.5. Temperature dependence of flexural strength

Fig. 5 shows typical stress-displacement curves of the ternary MGC obtained from the flexural test at 1873 K compared with those of a sintered ternary composite with the same chemical composition and an *a*-axis sapphire. All materials in Fig. 5 yield at 1873 K, but their behaviours are quite different. The Al_2O_3/YAG/ZrO_2 ternary MGC shows ductility under high stress, with a flexural strength of ~860 MPa which is around 57 times higher than the 15 MPa of the sintered ternary composite of the same composition and higher than the *a*-axis sapphire (approximately 450 MPa). Furthermore, the relative fracture energy of the Al_2O_3/YAG/ZrO_2 ternary MGC (which can be inferred from the area under the stress-strain curve) is much higher than those of the sintered ternary composite and the *a*-axis sapphire.

The fracture toughness of the ternary MGC at room temperature is approximately 5.2 MPa $m^{1/2}$, which is higher than the value of around 3 MPa $m^{1/2}$ for the Al_2O_3/YAG binary MGC and a little higher than 4–5 MPa $m^{1/2}$ for an advanced Si_3N_4 ceramic [21].

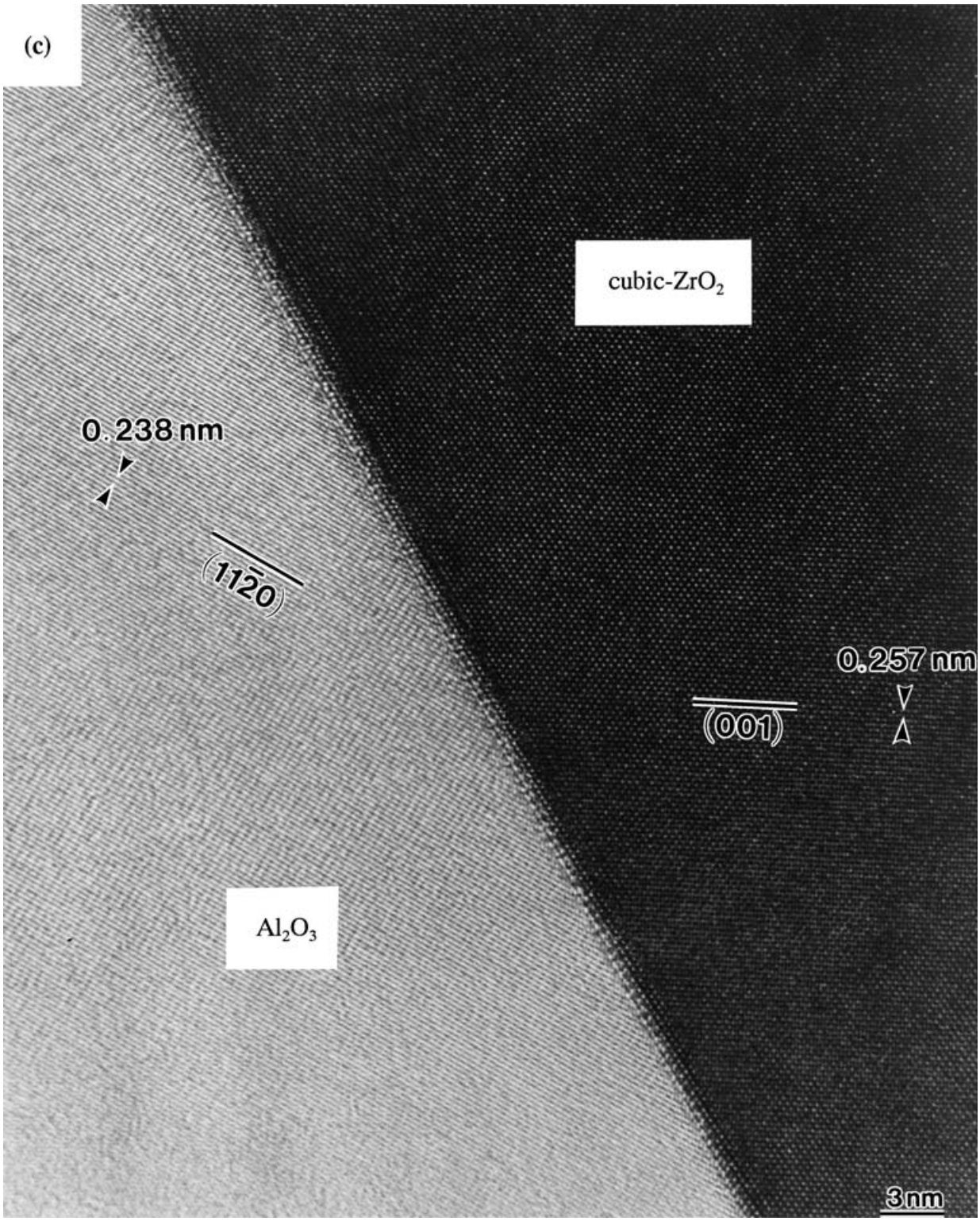

Figure 3 (*Continued.*)

The changes in flexural strength of the ternary MGC the sintered composite and an *a*-axis sapphire as a function of temperature are shown in Fig. 6. For comparison, the changes in flexural strength of Al_2O_3/YAG binary MGC [8, 11] and a Si_3N_4 advanced ceramic, which was recently developed for high temperature structural materials [22], are also shown in Fig. 6. There are significant differences. The flexural strength of the sintered composite increases slightly with a rise in temperature, but its strength falls precipitously above 1500 K. In the case of the *a*-axis sapphire, the flexural strength is the same or lower than that of sintered composite at room temperature, but its strength decreases progressively with increase in temperature until 1773 K, after which the it drops sharply. The Si_3N_4 advanced ceramic has the highest flexural strength of all of the materials at room temperature, but its strength decreases gradually with an increase of temperature above approximately 1000 K [22].

In contrast, the flexural strength of the ternary MGC increases gradually with temperature and its average flexural strength at 1873 K is approximately 800 MPa,

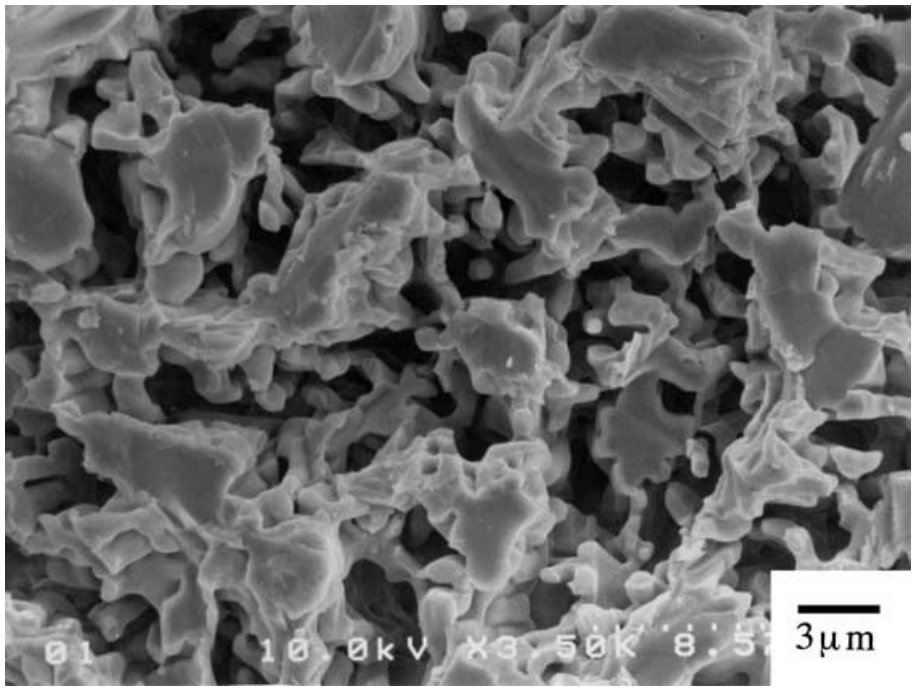

Figure 4 SEM micrograph showing the three-dimensional configuration of single-crystal YAG and single-crystal cubic-ZrO_2 in the Al_2O_3/YAG/ZrO_2 ternary MGC.

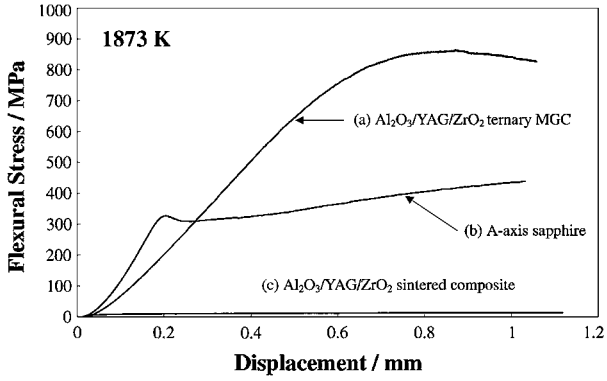

Figure 5 Typical stress-displacement curves in the three-point flexural test at 1873 K of (a) Al_2O_3/YAG/ZrO_2 ternary MGC compared with (b) *a*-axis sapphire and (c) Al_2O_3/YAG/ZrO_2 sintered composite.

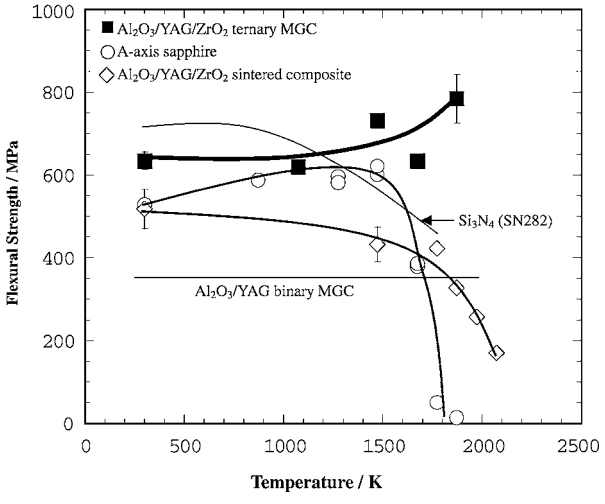

Figure 6 Temperature dependence of flexural strength of Al_2O_3/YAG/ZrO_2 ternary MGCs, *a*-axis sapphires and A-axis sapphire in comparison with Al_2O_3/YAG binary MGCs and Si_3N_4 (SN282) sintered advanced ceramics.

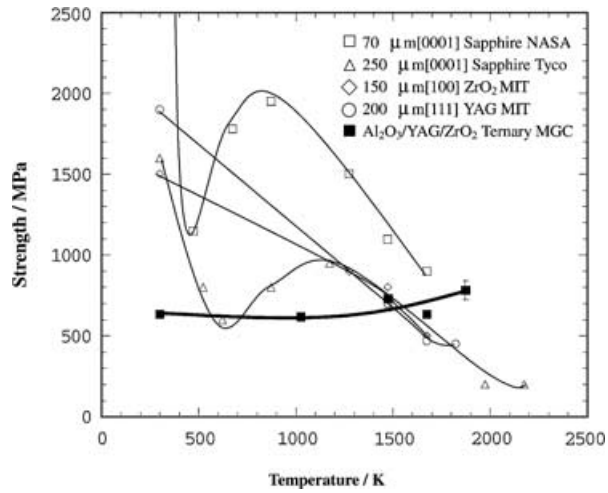

Figure 7 Change in strength of oxide single-crystal fibers and Al_2O_3/YAG/ZrO_2 ternary MGC as a function of temperature. (Tensile: all fibers, flexure: ternary MGC).

more than twice 350 MPa, the value of the Al_2O_3/YAG binary MGC [8, 11]. This difference between the binary and ternary MGCs is presumed to depend mainly on the dimensions of microstructure, with the finer microstructural dimensions being associated with higher strength at temperature. Further, the ternary MGC shows intergranular fracture in contrast to the transgranular fracture of the sintered composite with the same chemical composition.

Fig. 7 shows a summary of the temperature dependence of strength for sapphire fibers, a ZrO_2 fiber and a YAG fiber, i.e., the same materials as the constituent phases of the ternary MGC. For comparison, the flexural strength of the ternary MGC is also shown in Fig. 7. Above 1373 K, all the single-crystal oxide fibers show a progressive loss of strength due to creep rupture [23].

In contrast, the strength of the ternary MGC increases gradually with a rise in temperature and its strength at 1873 K is the same or higher than the [0001] single-crystal sapphire fibers, the [111] single-crystal YAG fiber, and [100] single-crystal zirconia fiber [23]. This is attributed to the ternary MGC's unique microstructure.

The maximum operating temperature of the present ternary MGC can be estimated to be ∼2023 K, which is much higher than that of Ni-based single-crystal cast superalloys (1323–1373 K) [24, 25], oxide ceramics (∼1300 K) [26, 27] and Si_3N_4 ceramics (∼1623 K) [28]. Therefore, this ternary MGC is expected to have wide application in mechanical engineering at very high temperatures in the future.

4. Conclusions

An Al_2O_3/YAG/ZrO_2 ternary MGC with a high-temperature flexural strength has been fabricated successfully by using a eutectic reaction of the Al_2O_3/Y_2O_3/ZrO_2 ternary system.

A compositional study was performed using a liquidus surface diagram calculated by the computer program Thermo-calc. The ternary MGCs have excellent high-temperature strength showing a slight increase in strength with increase in temperature from room temperature to 1873 K. The excellent high-temperature characteristics of the Al_2O_3/YAG/ZrO_2 ternary MGC are closely linked to such factors as: (1) the microstructure consisting of three-dimensionally continuous and complexly entangled single-crystal Al_2O_3, single-crystal YAG and fine single-crystal cubic-ZrO_2 without grain boundaries, (2) a fine microstructure with characteristic dimensions of around 2–3 μm for YAG, around 2–3 μm for Al_2O_3 and around 0.4–0.8 μm for ZrO_2 compared with 20–30 μm for the Al_2O_3/YAG binary MGC, (3) the interfaces between the Al_2O_3 and YAG, the Al_2O_3 and ZrO_2, the YAG and ZrO_2 which contain no amorphous phases.

Acknowledgment

This research was supported by NEDO as a part of the New Sunshine Program of Industrial Science and Technology, MITI.

References

1. The Japan Industrial Journal, September **12** (1994) 6.
2. D. VIECHNICKI and F. SCHMID, *J. Mater. Sci.* **4** (1969) 48.
3. T. MAH and T. A. PARTHASARATHY, *Ceram. Eng. Sci. Proc.* **11** (1990) 1617.
4. T. A. PARTHASARATHY, T. MAH and L. E. MATSON, *ibid.* **11** (1990) 1628.
5. *Idem.*, *J. Am. Ceram. Sci.* **76** (1993) 29.
6. A. SAYIR and S. C. FARMER, *Acta Mater.* **48** (2000) 4691.
7. J. Y. PASTOR, P. POZA, J. L. LORCA, J. I. PENA, R. I. MERINO and V. M. ORERA, *Mater. Sci. Eng.* A **308** (2001) 241.
8. Y. WAKU, N. NAKAGAWA, H. OHTSUBO, Y. OHSORA and Y. KOHTOKU, *J. Japan Inst. Metals* **59** (1995) 71.
9. Y. WAKU, H. OTSUBO, N. NAKAGAWA and Y. KOHTOKU, *J. Mater. Sci.* **31** (1996) 4663.
10. Y. WAKU, N. NAKAGAWA, T. WAKAMOTO, H. OHTSUBO, K. SHIMIZU and Y. KOHTOKU, *ibid.* **33** (1998) 1217.
11. *Idem.*, *ibid.* **33** (1998) 4943.
12. Y. WAKU and T. SAKUMA, *Journal of European Ceramic Society* **20** (2000) 1453.
13. Y. WAKU, N. NAKAGAWA, H. OHTSUBO, A. MITANI and K. SHIMIZU, *J. Mater. Sci.* **36** (2001) 1585.
14. Y. WAKU, S. SAKATA, A. MITANI and K. SHIMIZU, *Mat. Res. Innovat.* **5** (2001) 94.
15. ASTM Standard E399-90, Standard Test Method for Plain-Strain Fracture Toughness of Metallic Materials, Annual Book of ASTM Standard, Vol. 03.01 (ASTM, 1990) p. 407.
16. N. A. TOROPOV, I. A. BONDAR, F. YA. GALAKHOV, KH. S. NIKOGOSYAN and N. V. VINOGRADOVA, *Izv. Akad. Nauk SSSR, Ser. Khim.* (7) (1964) 1158.
17. G. R. FISCHER, L. J. MCNALLY and R. N. DOMAN, *J. Mater. Sci.* **16** (1981) 3447.
18. V. S. STUBICAN, R. C. HINK and S. P. RAY, *J. Amer. Ceram. Soc.* **61** (1978) 17.
19. D. R. CLARKE, *Ibid.* **62** (1979) 236.
20. J. ECHIGOYA, S. HAYASHI, K. SASAKI and H. SUTO, *J. Japan Inst. Metals* **48** (1984) 430.
21. I. BAR-ON, F. BARATTA and K. CHO, *J. Amer. Ceram. Soc.* **79** (1996) 2300.
22. M. YOSHIDA, K. TANAKA, T. KUBO, H. TERAZONE and S. TSURUZONE, in Proceedings of the international Gas Turbine and Aeroengine Congress and Exibition, Stockholm, Sweden, June 2–5, 1998 (The American Society of Mechanical Engineers, 1998) p. 1.
23. J. S. HAGERTY, J. SIGALOVSKY and E. L. COURTRIGHT in "Processing and Fabrication of Advanced Materials," edited by V. A. RAVI, T. S. SRIVATSAN and J. J. MOORE (TMS, Cleaveland, 1993) p. 297.
24. M. J. GOULETTE, in Proceeding of the Eighth International Symposium on Superalloys, 1996, edited by R. D. KISSINGER, D. J. DEYE, D. L. ANTON, A. D. CETEI, M. V. NATAL, T. M. POLLOCK and D. A. WOODFORD (TMS, Pennsylvania, 1996) p. 3.
25. G. L. Erickson, in Proceeding of the Eighth International Symposium on Superalloys, 1996, edited by R. D. KISSINGER, D. J. DEYE, D. L. ANTON, A. D. CETEI, M. V. NATAL, T. M. POLLOCK and D. A. WOODFORD (TMS, Pennsylvania, 1996) p. 35.
26. R. W. DAVIDGE and A. G. EVANS, *Mater. Sci. Eng.* **6** (1970) 281.
27. K. NIIHARA, *J. Ceram. Soc. Japan* **99** (1991) 974.
28. M. K. FERBER and H. T. LIN, in Proceedings of the International Gas Turbine and Aeroengine Congress and Exibition, Indianapolis, Indiana, June 7–10, 1999 (The American Society of Mechanical Engineers, 1999) p. 1.

Received 4 June 2001
and accepted 27 March 2002